


Article

Simulation Analysis with Randomly Distributed Multiple Projectiles and Experimental Study of Shot Peening

Wenxue Qian ^{1,2,*} , Shuanghui Huang ^{1,2}, Xiaowei Yin ^{3,*} and Liyang Xie ^{1,2}¹ School of Mechanical Engineering and Automation, Northeastern University, Shenyang 110819, China² Key Laboratory of Vibration and Control of Aero-Propulsion Systems, Ministry of Education, Northeastern University, Shenyang 110819, China³ School of Mechanical, Shenyang Institute of Engineering, Shenyang 110136, China

* Correspondence: wxqian@mail.neu.edu.cn (W.Q.); yinxw@sie.edu.cn (X.Y.); Tel.: +86-24-8368-3853 (W.Q.)

Abstract: Shot peening technology is used to improve the fatigue strength of materials and parts, and is one of the most effective surface engineering techniques to prolong fatigue life. In this paper, according to the finite element simulation analysis of shot peening, a randomly distributed multiple-shot finite element model was established. The superimposed effects of multiple projectile impact craters in shot peening are fully considered. The effects of shot velocity, shot peening angle and shot coverage on the residual stress field and surface roughness were studied. The alloy steel 20MnTiB, widely used in the automotive industry, was used as the raw material to process the specimens. The shot peening tests of different process parameters were carried out. The test results verified the correctness and accuracy of the random distribution model of multiple-shot. The shot-peening simulation model proposed in this paper allows a more accurate analysis of the effect of shot-peening parameters on the surface residual stress field and helps to quickly set the correct shot-peening process parameters. This paper further investigates the effect of shot peening parameters on fatigue life, providing a basis for the rational development of shot peening solutions.



Citation: Qian, W.; Huang, S.; Yin, X.; Xie, L. Simulation Analysis with Randomly Distributed Multiple Projectiles and Experimental Study of Shot Peening. *Coatings* **2022**, *12*, 1783. <https://doi.org/10.3390/coatings12111783>

Academic Editor: Michał Kulka

Received: 10 October 2022

Accepted: 18 November 2022

Published: 21 November 2022

Publisher's Note: MDPI stays neutral with regard to jurisdictional claims in published maps and institutional affiliations.



Copyright: © 2022 by the authors. Licensee MDPI, Basel, Switzerland. This article is an open access article distributed under the terms and conditions of the Creative Commons Attribution (CC BY) license (<https://creativecommons.org/licenses/by/4.0/>).

Keywords: multiple-shot peening; shot-peening coverage; residual stress; roughness; fatigue life

1. Introduction

20MnTiB is an alloy structural steel with good mechanical properties and process performance, mainly used to manufacture various gears, shafts and other key load-bearing components, which may suffer from fatigue failure in actual use due to the effect of alternating loads received. Shot peening is an effective means to improve its fatigue performance. Shot peening is an important surface treatment process. It uses high-speed particle flow to continuously impact the surface of the part, causing the surface to undergo plastic deformation, producing a cyclic hardening layer and residual compressive stress layer, thereby greatly improving the fatigue life of the part [1]. It is widely used in aerospace, military, automotive and other fields [2–4].

The process parameters affecting the shot peening effect include various factors such as projectile diameter, shot peening speed, and projectile coverage. In order to study the influence of these parameters on the shot-peening effect, scholars have established a variety of shot-peening models [5–9]. Al-Hassani [10,11] used the analytical method to study the distribution of compressive stress field and studied the static and dynamic impact models under the action of a single shot. The plastic deformation layers produced under static and dynamic loading are consistent. This study did not consider the different strain rate at the time of impact. Majzoubiet et al. [12] established a model in which a number of shots hit the workpiece according to a certain array position. The results show that the shot peening speed is not monotonically increasing for the shot peening effect, but there is an optimal speed, and this study did not consider the randomness of the position of the shot. Li et al. [13] applied the python programming language provided

by ABAQUS to establish a finite element model for the random distribution of the shot's spatial position. The experiment proved that this model is superior to the single-shot model. Gao et al. [14] established a multi-projectile simulation model, and designed a simulation test program to analyse the effect of each parameter, and fitted the relationship equation between each parameter and stress, and the results showed that the simulation model has high accuracy. Luan et al. [15] conducted a review and analysis of the effect of shot peening on the corrosion resistance of aluminium alloys, and the results showed that when the inappropriate shot peening parameters are adopted, the shot-peened surface integrity could be deteriorated, which further weakens the corrosion performance of the surface. Unal et al. [16] conducted a comparative study of various surface peening methods for AISI 1050, and the results showed that proper shot peening intensity is important for fatigue life improvement, and re-blasting can significantly reduce surface roughness, which is beneficial for improving the fatigue life of the material. Soyama et al. [17] showed that shot peening can significantly improve the fatigue properties of stainless steel. The fatigue strength of different shot peening methods is affected by surface roughness and work hardening. Matuszak et al. [18] compared conventional shot peening (RSP) and semi-random shot peening (SRSP) based on a finite element simulation approach. An experimental study was also carried out based on specimens of EN-AW 7075 aluminium alloy. It was found that conventional shot peening led to a reduction in surface roughness, while semi-random shot peening led to an increase in the degree of hardening of the surface layer. Wang et al. [19] used a femtosecond laser with ultra-high pulse density and ultra-low pulse energy to carry out nondestructive laser shot peening by combining the methods of experiment, finite element analysis and molecular dynamics simulation. Compared with traditional nanosecond laser shot peening, the surface roughness remained. The double temperature finite element analysis showed that no melting occurred during shot peening. Shen et al. [20] studied high-strength 7075-T651 aluminium alloy shot-peening using glass shot as the shot material. A random shot FE model was developed and the effects of shot number and spatial location on the residual stress field (RSF) were discussed. Hu et al. [21,22] used a modified three-dimensional random representative volume finite element model to systematically investigate the effects of model dimensions and thermal softening after shot peening on residual stresses, Almen strength, coverage and arc height. The necessity to consider thermal effects in the constituent material model of shot peening is also analysed. They conducted a systematic study combining experiments and multiple-shot finite element analysis to analyse the microstructural evolution and stress state of shot peened GH4169 superalloys at various strengths and coverage rates.

At present, the numerical models used in the peening research mainly include the single-shot peening model and the array-shot model. These models neglect the randomness of the shot position in the actual shot peening process, and there are not yet many applications of the stochastic distributed multi-shot model. In this paper, the APDL language is used to establish a randomly distributed multiple-shot impact model through parametric programming to more realistically simulate the shot-peening process. Based on the above model, the influence of shot-peening parameters on shot peening effect is analysed. The shot peening test was designed and was carried out under different shot peening parameters. The residual stress curves of different shot peening parameters were measured based on an X-ray residual stress tester. At last, the fatigue test of samples under different shot peening parameters was carried out, and the influence of shot peening parameters on fatigue life was analysed.

2. Finite Element Simulation Analysis

Numerical simulation is carried out by using the dynamic analysis and the LS-DYNA module. The target plate is a $3 \times 3 \times 1.2$ cuboid, and the shots are spheres with a diameter of 0.6 mm. The penalty factor value is 0.5. In order to improve the contact rigidity, the static friction coefficient is 0.2 and the friction coefficient is 0.15. Because the model is much less

than the actual size, it needs to apply vertical surface contact damping in order to avoid the impact of shock. The contact damping coefficient is:

$$\zeta = \frac{VDC\zeta_{crit}}{100} \quad (1)$$

The VDC is a viscous damping coefficient, which is defined as 20. ζ_{crit} is the critical damping coefficient, automatically calculated by the program.

$$\zeta_{crit} = 2m\omega \quad (2)$$

where m is the mass of the target plate and ω is the intrinsic frequency of the target plate.

The simulation analysis is based on the explicit dynamic analysis of LS-DYNA. The size of the target plate is $3 \times 3 \times 1.2 \text{ mm}^3$, the middle $1 \times 1 \times 1.2 \text{ mm}^3$ part meshes with a hexahedral mesh with 0.0025 mm edge length and the rest of the mesh size is 0.1 mm. The material is 20MnTiB and the material model is a Cowper-Symonds hybrid reinforced material model as in Equation (3).

$$\sigma_y = \left[1 + \left(\frac{\dot{\varepsilon}}{C} \right)^{1/p} \right] (\sigma_0 + \beta E_p \varepsilon_p^{eff}) \quad (3)$$

where $\dot{\varepsilon}$ is strain rate, C and p are strain rate parameters, β is the follow-up hardening parameter, E_p is plastic hardening modulus, E_{tan} is the tangential modulus, ε_p^{eff} is effective plastic strain, σ_0 is initial yield stress.

The position of shots is generated by random function, and the centre coordinates of shots are generated in the space of $1 \times 1 \times 5 \text{ mm}^3$. The non-reflecting boundary conditions are applied to the 4 sides and the bottom surface of the model, which can prevent the reflection at the boundary [23]. The finite element model with multiple randomly distributed shots is shown in Figure 1.

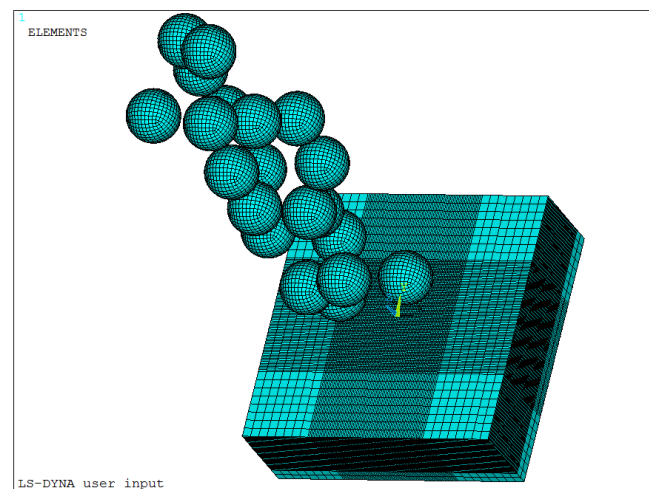


Figure 1. Finite element model with multiple randomly distributed shots.

Coverage was simulated by defining a shot speed of 60 m/s and vertical blasting with shot numbers of 10, 20, 30, 40 and 80. Residual stress distribution and surface roughness are simulated with a shot count of 80 and shot speeds of 40 m/s, 60 m/s, 80 m/s, 100 m/s and 120 m/s.

3. Experimental Procedure

3.1. Shot-Peening Test

The 20MnTiB is used as the test material, and its mechanical properties are shown in Table 1. The sample size is shown in Figure 2. The shot peening equipment is a VB100P air blasting machine, and the shot is made of cutting steel wire organized in spheres with a diameter of 0.6 mm. The spray distance is 180 mm.

Table 1. Mechanical properties of 20MnTiB.

Yield Strength σ_s /MPa	Tensile Strength σ_b /MPa	Elongation δ /%	Section Shrinkage ψ /%	Impact Absorption Energy KU_2 /J	Hardness/HRC
1200~1240	1330~1460	13.0~14.0	58.5~59.5	113~121	38~42

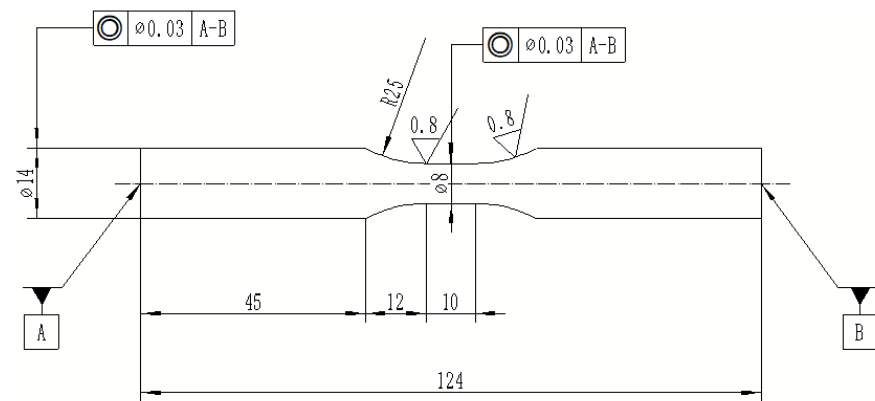


Figure 2. Sample size.

3.2. Residual Stress Test

Using X350A X-ray diffractometer to test surface residual stress [24–27]. Before the test, we first need to get a relatively flat cross-section by electrical discharge machining (EDM). In order to eliminate the machining residual stress, electropolishing technology is carried out for all samples after EDM. The sketch map is shown in Figure 3. The polishing solution is a mixing solution of 20% HClO₄ and 80% alcohol. After electrolytic polishing, residual stress σ_x along the depth direction is tested using an X-ray diffractometer, and the detailed parameters are shown in Table 2.

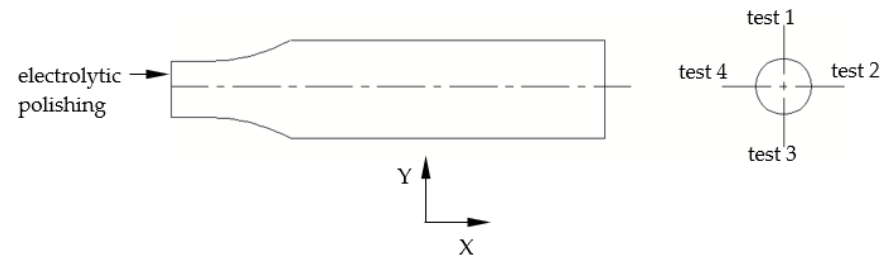


Figure 3. Sketch map of electrolytic polishing and measuring position.

Table 2. Parameters of the X-ray diffractometer.

Measuring method: roll fixing method Ψ	Ψ angle: 0.0°, 24.2°, 35.3°, 45.0°	2 θ scan end angle: 146°
Diameter collimator: $\Phi 3$ mm	Stress constant: −318 MPa/angle	2 θ scan step: 0.10°
The method for determining peak positions: cross correlation method	Diffraction plane: (211)	X-ray tube voltage: 30 KV
Target shooting: Cr K α	2 θ scan start angle: 166°	X-ray tube current: 6.7 mA

4. Results and Discussion

4.1. Simulation Results and Discussion

4.1.1. Influence of Shot-Peening Coverage on Residual Stress and Surface Roughness

The coverage is simulated by defining the number of randomly distributed shots. The greater the number, the greater the shot coverage. Define the shot peening speed as 60 m/s, vertical injection, the number of shots is 10, 20, 30, 40, 80, respectively, and $41 \times 41 = 1681$ paths are defined along the depth in the collision area. The node stress at each layer is averaged to obtain the residual stress σ_x along the depth direction.

Figure 4 shows with the increase of coverage, the residual compressive stress of the surface increases gradually, and the residual compressive stress layer depth increases correspondingly, which is eventually stabilized at around 0.56 mm. The maximum residual compressive stress increases with the increase of the number of shots, and the value is no longer increased at a number of 40, eventually stabilizing at about 730 MPa. Therefore, when the number of shots reaches a certain value, that is, the peening coverage reaches a certain value, the residual stress distribution is close to saturation. The effect of shot peening will not be enhanced even if shot peening is continued.

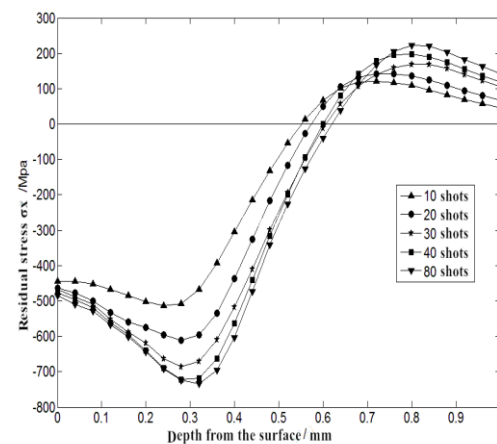


Figure 4. Residual stress distribution along depth.

Figures 5 and 6 show the surface morphology and surface displacement after shot peening when the number of shots is 80. These results are the same as [28]. According to the shot peening standard, the surface roughness of shot peening is evaluated by R_a [29]. By calculating the node displacement of the target plate surface along the Z direction, the value of the roughness is obtained by using the least square line as the datum line. Figure 5 respectively shows the change of the surface roughness when the number of shots is 10, 20, 30, 40, 60, 80, 100, and 120.

Figure 7 shows with the increase in the number of shots, surface roughness gradually increases. When the number of shots is 80, roughness decreases slightly. This is because shot peening has a levelling effect on the crater formed early when the coverage rate reached 100% [30]. With continued shot peening, the value of the roughness increases slightly and tends to saturation. It can be seen that there is an optimal value of the shot coverage rate. After reaching a certain value, the roughness value remains basically the same, and the shot peening for a long time has no significant influence on the surface roughness of the test piece.

4.1.2. Influence of Different Shot Speeds on Residual Stress and Surface Roughness

Figures 8 and 9 show the residual stress distribution and the value of roughness when the number of shots is 80, the shot speed is 40 m/s, 60 m/s, 80 m/s, 100 m/s and 120 m/s, respectively.

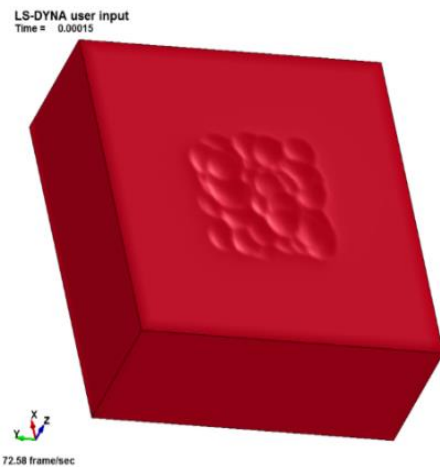


Figure 5. Surface morphology after shot peening.

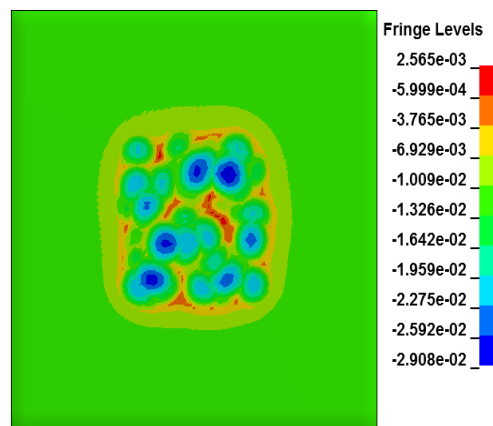


Figure 6. Surface displacement after shot peening.

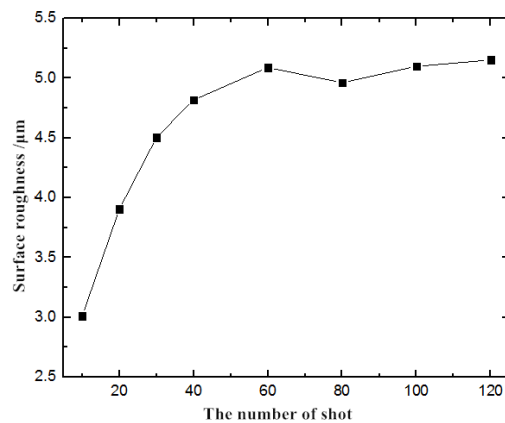


Figure 7. Roughness under different numbers of shots.

As can be seen from Figure 8, as the velocity of the shot increases, the surface residual compressive stress value gradually decreases, the depth of the pressure layer gradually increases, the peak value of the compressive stress increases first and then decreases, and the surface roughness also increases. Therefore, it is not that the higher the shot speed (pressure), the better the shot peening effect; rather, there is an optimum speed (pressure) value.

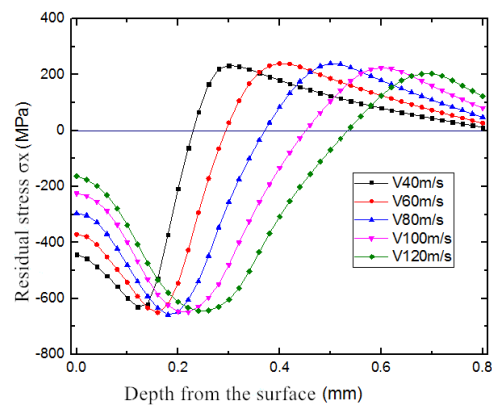


Figure 8. Residual stress distribution under different shot speeds.

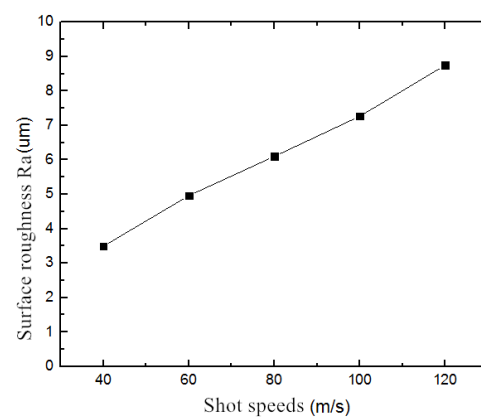


Figure 9. Surface roughness under different shot speeds.

4.2. Test Results and Discussion

4.2.1. Effect of Shot-Peening on Residual Stress Distribution

The measured residual stress distribution under different shot peening pressure is shown in Figure 10. As shown in the picture, with the increase of peening pressure, surface residual compressive stress is gradually reduced, and the depth of the residual compressive stress layer gradually increases. The maximum compressive residual stress is -718 MPa, -747 MPa, -728 MPa, separately. The value first increases and then decreases and these are consistent with the simulation results in Figure 6. This result is similar to that of the literature [31]. Figure 11 shows a comparison of the test shot peening residual stresses with the simulated shot peening residual stresses. Under these blasting parameters, there is a blast coverage of 200%, a blast angle of 90° , a test shot pressure of 0.2 MPa and a simulated shot speed of 60 m/s. The surface residual compressive stress values of the simulation results are 2.7% less than the test results. The peak value of residual compressive stress is only 1.7% less than the test result, so this model can better simulate the actual shot-peening process.

4.2.2. Effect of Shot-Peening on Roughness

Use a JXD-B reading microscope to observe the surface morphology of shot peening samples. The surface roughness measurement is carried out by using the MiCROMEASUR2 3D profile of the French STIL company.

(1) The effect of different shot peening pressure on the roughness

Figures 12 and 13 separately show the surface morphology and roughness after shot peening when the pressures are 0.1 MPa, 0.2 MPa and 0.3 MPa respectively, and the magnification of the image is $25\times$.

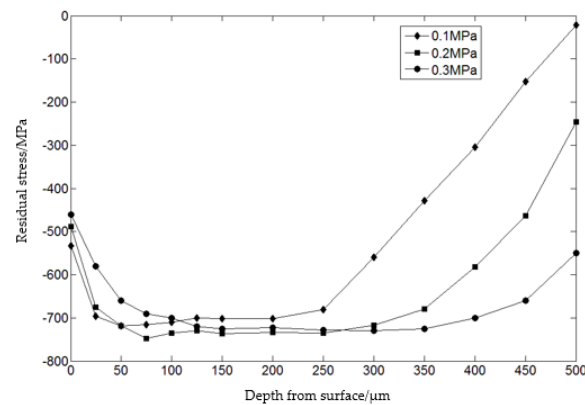


Figure 10. Distribution of residual stress.

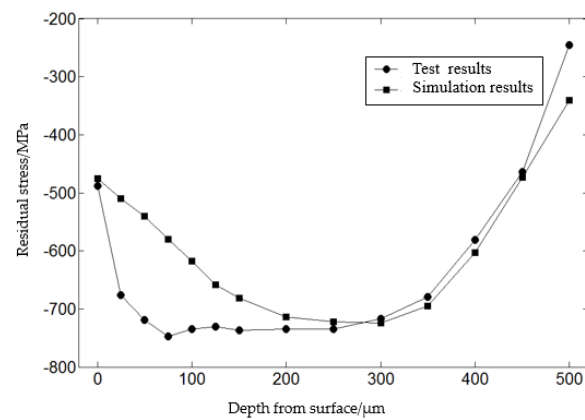


Figure 11. Comparison of the numerical simulation results and the experimental result.

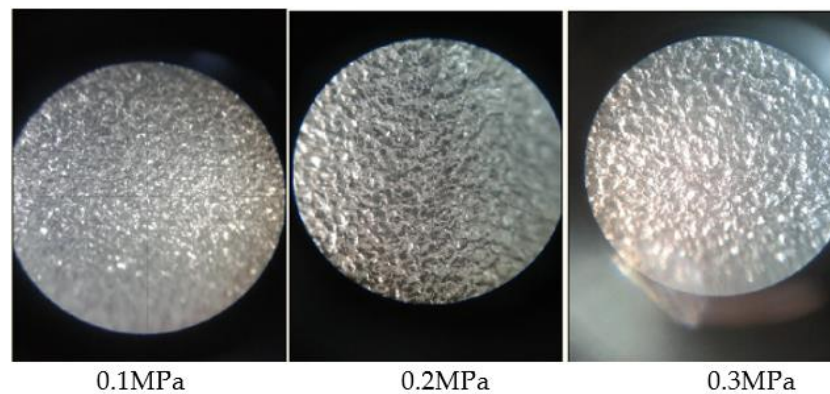


Figure 12. Surface morphology of the shot peening under different pressures.

As shown in Figure 12, with the increase of shot peening pressure, the surface morphology of the sample is rougher, and surface roughness also increases. The experimental results are consistent with Figure 9.

(2) The effect of different injection angles on the roughness

Figures 14 and 15 separately show the surface morphology and roughness after shot peening when the pressure is 0.1 MPa and the spray angles are 90° and 60° ; the magnification of Figure 14 is $25\times$.

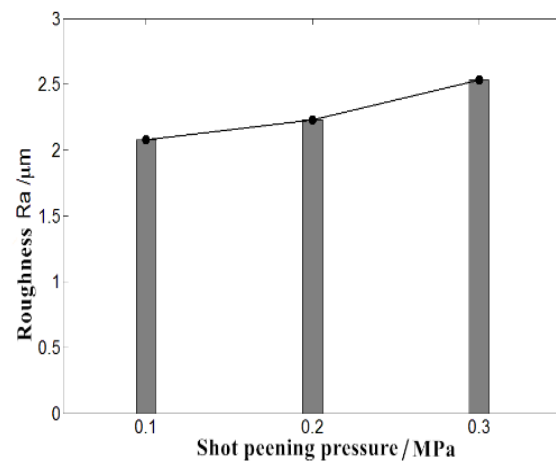


Figure 13. Roughness after shot peening under different pressures.

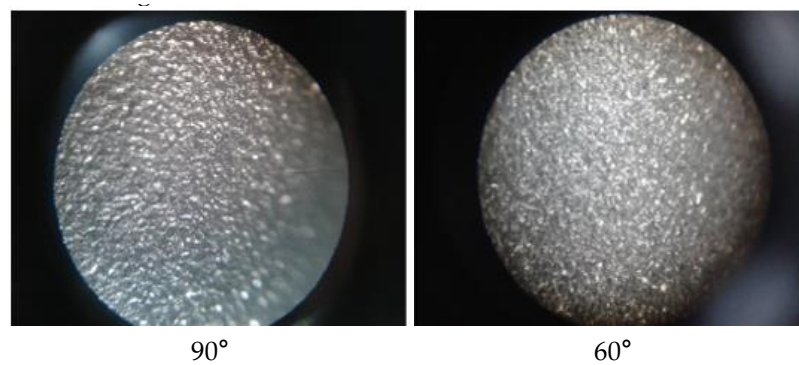


Figure 14. Surface morphology under different spray angles.

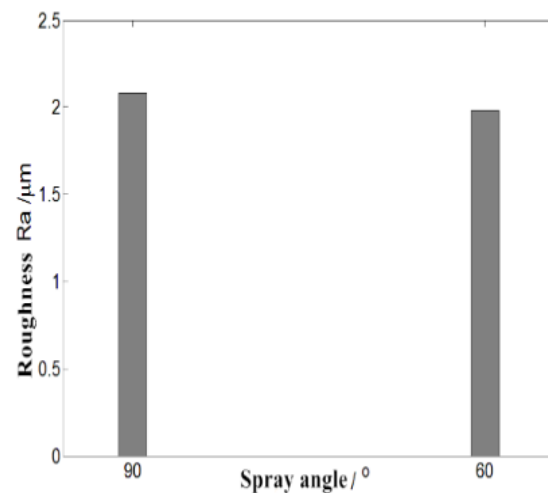


Figure 15. Surface roughness under different spray angles.

Figure 15 shows that the surface roughness at 60° is slightly less than the surface roughness at 90°, mainly because the smaller the spray angle, the corresponding normal velocity component will be reduced, and the depth of the crater will be reduced. Moreover, due to the tangential velocity component, subsequent shots will have a levelling effect on the previous craters, and the roughness will be reduced further. However, due to the smaller normal speed, the maximum residual compressive stress and the compressive stress layer are smaller; thus, the strengthening effect is reduced.

4.2.3. Effect of Shot-Peening on Fatigue Life

A fatigue test is carried out by using the SHIMADZU EHF-EM/EV series electro-hydraulic servo fatigue testing machine. The fatigue lives under different stress levels are measured when the stress ratio is -1 .

(1) Fatigue lives under different shot-peening pressures

Figure 16 shows respectively the fatigue lives of unpeened specimens and peened specimens under 0.1 MPa, 0.2 MPa, and 0.3 MPa shot peening pressure separately, and the stress level is 600 MPa.

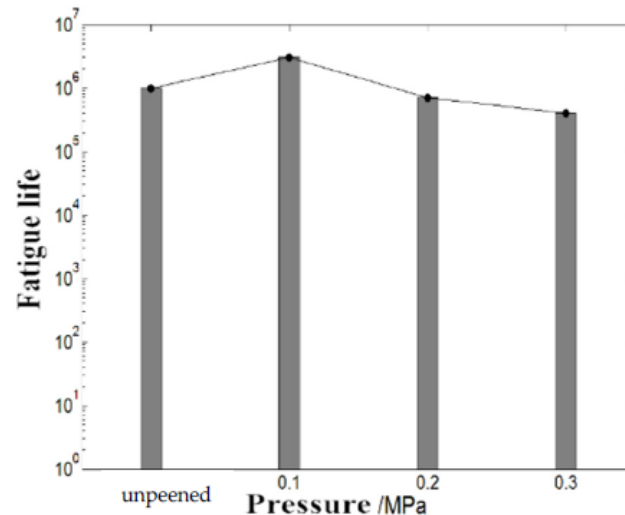


Figure 16. Fatigue lives of different peening pressures under 600 MPa stress level.

As shown in the picture, when the stress level is 600 MPa, the fatigue life of an unpeened specimen is 1×10^6 . When shot peening pressure is 0.1 MPa, the fatigue life is greatly improved to 3×10^6 , which is improved by 200%. However, when the pressures are 0.2 MPa and 0.3 MPa, the fatigue lives are decreased. This is because excessive shot peening pressure results in large roughness, and even the specimen surface produces a micro-crack, which reduces the fatigue life. So, the shot peening process must select a suitable peening pressure.

(2) Fatigue lives under different shot peening coverage rate

Figure 17 shows respectively the fatigue lives of unpeened specimens and peened specimens when the coverage rates are 80% and 200%, separately, in the case of shot peening pressure is 0.1 MPa.

As shown in Figure 17, when the peening coverage is 80%, the fatigue life is reduced by 50% compared to unpeened specimens under 600 MPa stress level, and the fatigue life is reduced by 67% compared to unpeened specimens under 700 MPa stress level. When shot peening coverage is 200%, the fatigue lives under 600 MPa and 700 MPa stress levels are increased by 200% and 33%, separately. Therefore, it is concluded that when the peening coverage is less than 100%, the fatigue life is decreased. The main reason is that the residual tensile stress is generated on the surface, and the residual stress distribution along the depth direction is not uniform, which reduces the fatigue life.

(3) Effect of different spray angles on fatigue lives

Figure 18 shows respectively the fatigue lives of unpeened specimens and peened specimens when the spray angles are 60° and 90° , separately, when shot peening pressure is 0.1 MPa.

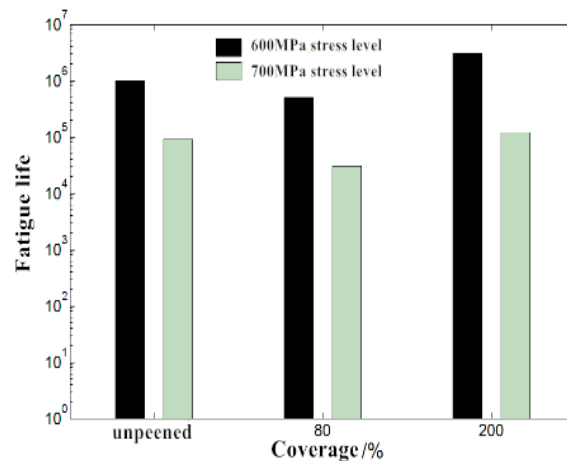


Figure 17. Effect of different shot peening coverage rates on fatigue lives.

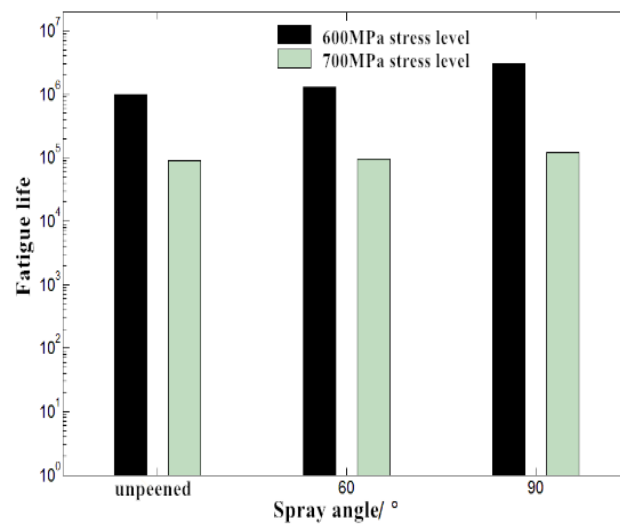


Figure 18. Effect of different spray angles on fatigue lives.

From Figure 18, it can be seen that the fatigue life of the peened specimens at 60° and 90° has a certain increase compared to that without shot peening. However, the fatigue life under 90° spray angle is improved significantly. Although the roughness at the 60° spray angle is smaller than that at the 90° spray angle, the fatigue life is greatly improved under the 90° spray angle. That is because the spray angle is vertical so that greater residual compressive stress is produced on the surface of the sample, and the surface is strengthened.

5. Conclusions

In this paper, a multiple-shot random distribution model is established to simulate the shot peening process, and the following conclusions are drawn combined with experimental study:

- (1) The simulation results of the multiple-shot random distribution model are basically consistent with the experimental results, which can better simulate the process of shot peening.
- (2) With the increase of peening coverage, the depth of the compressive residual stress layer increases and surface roughness becomes larger. However, the residual stress field distribution and surface roughness value become stable when the coverage rate reaches a certain value. The following shot peening will not make it more useful. However, the fatigue life will be reduced when the coverage rate is less than 100%, so the coverage rate must be at least 100%.
- (3) With the increase of peening pressure, surface residual compressive stress decreases gradually, and the depth of the residual compressive stress layer increases. Surface

roughness becomes larger, correspondingly, and the peak pressure force first increases and then decreases. Nevertheless, the surface of parts will generate micro-cracks due to excessive pressure, which reduces the fatigue life.

For residual stress testing, different stripping methods may have an effect on the residual stress test results and need to be further investigated in subsequent work.

Author Contributions: Conceptualization and methodology, W.Q.; data curation, S.H.; writing—original draft preparation, W.Q. and X.Y.; writing—review and editing, W.Q.; project administration, L.X. All authors have read and agreed to the published version of the manuscript.

Funding: This work was partially supported by the National Natural Science Foundation of China (Grant No. 52175131), the National Science and Technology Major Project of the Ministry of Science and Technology of China (Grant No. J2019-IV-0002-0069, J2019-IV-0016-0084) and the Natural Science Foundation of Liaoning Province of China (Grant No. 2021-MS-269).

Institutional Review Board Statement: Not applicable.

Informed Consent Statement: Not applicable.

Data Availability Statement: All the data used in this study can be found in the article.

Conflicts of Interest: The authors declare no conflict of interest.

References

- Dong, X.; Zhang, H.; Duan, X. Finite element simulation of residual stress field with water jet peening strengthening. *Chin. J. Mech. Eng.* **2010**, *46*, 189–194. [[CrossRef](#)]
- Concli, F. Numerical study of the impact of shot peening on the tooth root fatigue performances of gears using critical plane fatigue criteria. *Appl. Sci.* **2022**, *12*, 8245. [[CrossRef](#)]
- Huang, H.; Niu, J.; Xing, X.; Lin, Q.; Chen, H.; Qiao, Y. Effects of the shot peening process on corrosion resistance of aluminum alloy: A review. *Coatings* **2022**, *12*, 629. [[CrossRef](#)]
- Villegas, J.C.; Shaw, L.L. Nanocrystallization Process and mechanism in a nickel alloy subjected to surface severe plastic deformation. *Acta Mater.* **2009**, *57*, 5782–5795. [[CrossRef](#)]
- Heydari, A.; Bagherifard, S.; Bradanini, A.; Duó, P.; Henze, S.; Taylor, B.; Guagliano, M. Application of shot peening to case-hardened steel gears: The effect of gradient material properties and component geometry. *Surf. Coat. Technol.* **2020**, *398*, 126084. [[CrossRef](#)]
- Tu, F.; Delbergue, D.; Klotz, T.; Bag, A.; Miao, H.; Bianchetti, C.; Brochu, M.; Bocher, P.; Levesque, M. Discrete element-periodic cell coupling model and investigations on shot stream expansion, Almen intensities and target materials. *Int. J. Mech. Sci.* **2018**, *145*, 353–366. [[CrossRef](#)]
- Sanjurjo, P.; Rodríguez, C.; Peñuelas, I.; García, T.E.; Belzunce, F.J. Influence of the target material constitutive model on the numerical simulation of a shot peening process. *Surf. Coat. Technol.* **2014**, *258*, 822–831. [[CrossRef](#)]
- Gariépy, A.; Miao, H.Y.; Lévesque, M. Simulation of the shot peening process with variable shot diameters and impacting velocities. *Adv. Eng. Softw.* **2017**, *114*, 121–133. [[CrossRef](#)]
- Yang, F.; Chen, Z.; Meguid, S.A. Effect of initial surface finish on effectiveness of shot peening treatment using enhanced periodic cell model. *Int. J. Mech. Mater. Des.* **2014**, *11*, 463–478. [[CrossRef](#)]
- Al-Hassani, S. Mechanical aspects of residual stress development in shot peening. In Proceedings of the 1st International Conference on Shot Peening (ICSP1), Paris, France, 14–17 September 1981; pp. 583–602.
- Al-Hassani, S. An engineering approach to shot peening mechanics. In Proceedings of the 2nd International Conference on Shot Peening (ICSP2), Chicago, IL, USA, 14–17 May 1984; pp. 275–281.
- Majzoubi, G.H.; Azizi, R.; Alavi Nia, A. A three-dimensional simulation of shot peening process using multiple shot impacts. *J. Mater. Process. Technol.* **2005**, *164*, 1226–1234. [[CrossRef](#)]
- Li, Y.; Lei, L.; Zeng, P. Shot stream finite element model for shot peening numerical simulation and its experiment study. *Chin. J. Mech. Eng.* **2011**, *47*, 43–48. [[CrossRef](#)]
- Gao, Z.; Liao, K.; Chen, J. Surface characteristic function of al alloy after shot peening. *Coatings* **2021**, *11*, 160. [[CrossRef](#)]
- Luan, W. Recent trends on surface modification technology of shot peening. *China Mech. Eng.* **2005**, *16*, 1405–1409.
- Unal, O.; Maleki, E.; Karademir, I.; Husem, F.; Efe, Y.; Das, T. Effects of conventional shot peening, severe shot peening, re-shot peening and precised grinding operations on fatigue performance of AISI 1050 railway axle steel. *Int. J. Fatigue* **2022**, *155*, 106613. [[CrossRef](#)]
- Soyama, H. Comparison between the improvements made to the fatigue strength of stainless steel by cavitation peening, water jet peening, shot peening and laser peening. *J. Mater. Process. Technol.* **2019**, *269*, 65–78. [[CrossRef](#)]
- Matuszak, J.; Zaleski, K.; Skoczylas, A.; Ciecielag, K.; Kecik, K. Influence of semi-random and regular shot peening on selected surface layer properties of aluminum alloy. *Materials* **2021**, *14*, 7620. [[CrossRef](#)]

19. Wang, P.; Cao, Q.; Liu, S.; Peng, Q. Surface strengthening of stainless steels by nondestructive laser peening. *Mater. Des.* **2021**, *205*, 109754. [[CrossRef](#)]
20. Sheng, X.; Xia, Q.; Cheng, X.; Lin, L. Residual stress field induced by shot peening based on random-shots for 7075 aluminum alloy. *Trans. Nonferrous Met. Soc. China* **2012**, *22*, s261–s267. [[CrossRef](#)]
21. Hu, D.; Gao, Y.; Meng, F.; Song, J.; Wang, R. Experimental and Numerical Analysis of Microstructures and Stress States of Shot-Peened GH4169 Superalloys. *Metall. Mater. Trans. A* **2018**, *49*, 1397–1409. [[CrossRef](#)]
22. Hu, D.; Gao, Y.; Meng, F.; Song, J.; Wang, Y.; Ren, M.; Wang, R. A unifying approach in simulating the shot peening process using a 3D random representative volume finite element model. *Chin. J. Aeronaut.* **2017**, *30*, 1592–1602. [[CrossRef](#)]
23. Zhang, H.; Zhang, Y.; Wu, Q. Numerical simulation of shot-peening process and impact effect. *Acta Metall. Sin.* **2010**, *46*, 111–117. [[CrossRef](#)]
24. Xiao, X.; Tong, X.; Gao, G.; Zhao, R.; Liu, Y.; Li, Y. Estimation of peening effects of random and regular peening patterns. *J. Mater. Process. Technol.* **2018**, *254*, 13–24. [[CrossRef](#)]
25. Yang, Q.; Cheng, J.; Guan, H.; Tan, W.; Zhang, Y. Investigation of wet shot peening on microstructural evolution and tensile-tensile fatigue properties of Ti-6Al-4V alloy. *Mater. Chem. Phys.* **2022**, *291*, 126635. [[CrossRef](#)]
26. Li, R.; Liu, D.; Wei, Z.; Xuan, L.; Qiao, M.; Xia, M. Influence of shot peening and surface integrity on the fatigue properties of 300m steel. *Mech. Sci. Technol. Aerosp. Eng.* **2011**, *30*, 1418–1421.
27. Li, J. Determination of superficial stress-strain relationship with x-ray diffraction technique. *Chin. J. Mater. Res.* **1998**, *12*, 287–290.
28. Zhang, Y.; Zhang, Z.; Liu, J. The distribution of residual stress along the depth under different shot peening process. *J. Beijing Univ. Technol.* **2009**, *35*, 1584–1590.
29. Yang, Y.; Qiao, M.; Zhang, W. Influence of shot peening parameters on the residual stress field. *China Surf. Eng.* **2009**, *22*, 45–48.
30. Zhu, X. Application Study of Shot Peening Process on Parts Surface. *Mod. Veh. Power* **2013**, *2*, 38–40.
31. Gundgire, T.; Jokiaho, T.; Santa-aho, S.; Rautio, T.; Järvenpää, A.; Vippola, M. Comparative study of additively manufactured and reference 316 L stainless steel samples—Effect of severe shot peening on microstructure and residual stresses. *Mater. Charact.* **2022**, *191*, 112162. [[CrossRef](#)]